Multi-reaction-channel fitting calculations in a coupled-channel model

Scholten, O.; Usov, A.

Published in:
Pramana-Journal of physics

DOI:
10.1007/s12043-010-0110-z

Publication date:
2010

PRAMANA
— journal of
physics

Vol. 75, No. 2
August 2010
pp. 215–224

Multi-reaction-channel fitting calculations in a coupled-channel model: Photoinduced strangeness production

O SCHOLTEN[1,*] and A USOV[1,2]
[1]Kernfysisch Versneller Institute, University of Groningen, Groningen, The Netherlands
[2]University of Leiden, Leiden, The Netherlands
[*]Corresponding author. E-mail: scholten@kvi.nl

Abstract. To describe photo- and meson-induced reactions on the nucleon, one is faced with a rather extensive coupled-channel problem. Ignoring the effects of channel coupling, as one would do in describing a certain reaction at the tree level, invariably creates a large inconsistency between the different reactions that are described. In addition, the imaginary parts of the amplitude, which are related through the optical theorem, to total cross-sections, are directly reflected in certain polarization observables. Performing a full coupled-channel calculation thus offers the possibility to implement the maximum number of constraints. The drawback one is faced with is to arrive at a simultaneous fit of a large number of reaction channels. While some of the parameters are common to many reactions, one is still faced with the challenge to optimize a large number of parameters in a highly non-linear calculation. Here we show that such an approach is possible and present some results for photoinduced strangeness production.

Keywords. Photoinduced strangeness production; polarization observables; baryon resonances; k-matrix; chi-square fitting.

PACS Nos 12.10.-g; 13.60.Le; 13.75.Gx; 13.75.Jz; 14.20.Gk; 25.80.-e

1. Introduction

To describe channel coupling effects we adopt the K-matrix formalism. The K-matrix formalism is a very powerful scheme for performing coupled-channel calculations in a large model space based on an effective Lagrangian formulation. Here we present a short overview of the K-matrix approach: a more detailed description can be found in refs [1–5]. The K-matrix formalism generates an infinite, non-perturbative set of loop corrections. A number of basic symmetries like gauge invariance, unitarity and crossing symmetry are conserved in this formalism.

In the K-matrix formalism the scattering matrix is written as

$$T = \frac{K}{1 - iK}. \tag{1}$$

It is easy to check, that the resulting scattering amplitude $S = 1 + 2iT$ is unitary provided that K is Hermitian. The expression in (1) results from a re-summation of an infinite-geometrical series of loop diagrams. This simple re-summation is possible since only the pole contributions are considered in the loop integrals. These correspond to two on-mass-shell intermediate particles which are the minimal set of diagrams to ensure two-particle unitarity. The omitted real parts of the loop integrals can be absorbed as real vertex functions and self-energies [6,7]. We have however chosen to work with purely phenomenological form factors to model these loop corrections that are not explicitly accounted for in the formalism. An alternative procedure to account for the real-loop corrections is offered by the approach of refs [8,9].

The strength of the K-matrix procedure is that, in spite of its simplicity, it satisfies several symmetries and conservation laws [10]. For a Hermitian kernel the resulting amplitude is unitary. If the kernel is gauge invariant the full amplitude obeys gauge invariance, and if in addition the kernel is crossing symmetric the full amplitude is crossing symmetric. These properties are crucial for the proper behaviour of the scattering amplitude in the low-energy limit. Since a full re-summation is performed to obtain the scattering matrix, all non-perturbative coupled-channel effects automatically are accounted for. This implies – for example – that resonance-like structures may be generated in the cross-section for a particular channel which are solely generated to the coupling to a third channel. Some recent examples of this can be found in refs [2,11,12]. Also, as a result of the channel coupling, the resonances generate widths which are consistent with their coupling to all channels included in the model space. For some resonances, such as the Δ and the $S_{11}(1535)$, this corresponds to their total width. Other resonances, particularly the high-lying ones, may have important decay branches to states that are not included in the model basis. To account for this we have added an explicit dissipative part to the corresponding propagators [3].

The kernel in the K-matrix approach is built from tree-level diagrams using an effective Lagrangian. A complete set of s-, t-, and u-channel diagrams are included. As basis we consider only stable particles or narrow resonances in two-body final states, $N\gamma$, $N\pi$, $N\eta$, ΛK, ΣK, $N\phi$, and recently [12] $\Lambda(1520)K$. To investigate the effects of coupling to more complicated states, we have also included the $N\rho$-final state. As was shown in ref. [1], inclusion of the ρ-channel has a strong influence on the pion sector. Also for some of the strangeness production channels the effect of including the ρ-channel clearly affects the spectra. All reactions within this model space are calculated self-consistently.

As mentioned before, form factors are to be included in this approach to account for the real parts of the loop corrections [6,13]. Phenomenologically the form factors are necessary to suppress the contributions of the Born terms at high energies. In a phenomenological approach, which we are following here, the form factors are not known *a priori* and thus introduce arbitrariness in the model. For simplicity we limit ourselves to dipole form factors in the s-, u- and t-channels,

$$F_m(s) = \frac{\lambda^2}{\lambda^2 + (s - m^2)^2} \ , \tag{2}$$

where m is the mass of the propagating particle and λ is the cut-off parameter. For the u-channel form factors we have introduced an additional suppression factor [1]

$$H_m(u) = \frac{u\lambda^2}{\big(\lambda^2 + (u - m^2)^2\big)m^2}. \tag{3}$$

Without this additional suppression factor the contribution of the u-channel gives rise to a strong backward peaking of the cross-section at large energies. To limit the overall number of parameters we have taken the same cut-off value ($\lambda = 1.2$ GeV^2), for all form factors.

Inclusion of form factors will in general break the electromagnetic gauge invariance of the model. Since any gauge-invariance restoration procedure is model-dependent [1], one may obtain strongly different predictions for photoinduced cross-sections, even at the level of Born contributions. Therefore, the choice of a procedure to be adopted is guided by its ability to describe the experimental data. It was found that the gauge-restoration procedure of Davidson and Workman [14] (DW) provided the best description of the data on $K - \Sigma$ photoproduction. The difference between the various gauge-restoration approaches can be expressed in terms of contact terms. The use of an effective Lagrangian formalism allows to include these contact terms with coupling constants that can be treated as free parameters. Thus, the model dependence can be kept to a minimum. A detailed description of our model can be found in refs [1,2].

The model describes a very large number of reaction channels and there are thus a sizable number of coupling constants that have to be adjusted to data. We present here the implementation of an automated fit procedure. It is shown that even in a coupled-channel framework, not all phase shifts can be determined uniquely in the absence of a complete set of polarization observables.

2. Parameter fitting

For a correct interpretation of the data in terms of resonances [15–20] it is important to ascertain the uniqueness of the extracted parameters. For this purpose we have implemented an automatic χ^2-fitting option. The advantage of such an approach is that it allows for an unbiased determination of the parameters.

Fitting of large coupled-channel calculation to experimental data is significantly more complicated than fitting of a simple tree-level model due to the high degree of non-linearity. Since changing parameters in one particular channel may affect the results in another, one can no longer split the set of parameters in smaller sub-sets where each is fitted to a particular reaction. In addition, one has to fit many reaction channels simultaneously and, albeit that several have parameters in common, this amounts to a large number of parameters. On the other hand, there is a much larger database which can be used in the fit. This allows – in principle – for a more accurate determination of the parameters, but necessitates more extensive calculations. To be able to perform the necessary calculations, one should devote special attention to optimize the code. In the next section this point will be addressed.

In optimizing the calculations we decided to treat the 'light' channels, π–N and γ–N, as a separate class from the kaon-production channels. In the calculations we assume that these lighter channels decouple from the heavier ones and can thus be treated as fixed, of course provided that the parameters for pion and photon

couplings are taken constant. This has the effect of cutting on calculation time (the corresponding matrix elements have to be calculated only once and stored for re-use in subsequent fitting iterations) as well as drastically reducing the number of fitting parameters since the pion and photon couplings have been obtained from earlier fits to π–N phase shifts and photoproduction amplitudes. This leaves just the $K-\Lambda$ and $K-\Sigma$ coupling constants in Born terms and resonances as well as contact terms as free parameters. At the end of the calculations, one should of course verify that the results in the π–N and the γ–N sectors have indeed remained approximately constant.

Another extremely important optimization concerns the calculation of the value of χ^2 which needs to be re-evaluated many times during the iteration process. In the traditional approach, we should evaluate the observables for every data point to calculate the contribution to the χ^2 value. The obvious way to improve this process is to bin the data into relatively small energy bins and to calculate χ^2 for every energy bin. Since different experiments use different bin sizes, this is not very practical and in our calculation we went a step further and defined an energy grid for the calculation of a complete set of partial-wave amplitudes. Next we define an interpolating spline for each partial wave and use it to extract the partial-wave decomposition for the specific energy where the data have been measured. As the partial waves for kaon photoproduction channels are a relatively smooth function of energy, this approach gives surprisingly good results even with sparse energy grids. With all these optimizations in place, we have gained about one order of magnitude in computing time.

3. The fitting calculations

The minimization technique we use is similar to the multistage minimization technique described in ref. [21]. The first stage of the minimization process consists of genetic algorithm search, which is capable of efficiently covering the full parameter space. As the second stage we use a gradient minimization scheme as implemented by DN2FB algorithm from the PORT3 package [22]. We have found the DN2FB algorithm to be far superior to the traditional Minuit package in terms of performance. DN2FB works on the basis of the first derivatives only and for this reason it is much faster than Minuit. The use of DN2FB was imperative since we are dealing with a much larger number of parameters, a much higher degree of non-linearity and more time-consuming calculations than what was needed in the work of ref. [21]. Only in the final stage of the minimization procedure, close to the minimum, we use the Minuit package to obtain the final values of parameters and to extract the correlation matrix for the parameters.

Such a staged approach has a number of advantages. The use of a genetic algorithm is extremely efficient in finding the first approximation to the minimum point, while the DN2FB minimizer allows to quickly refine the found minimum. This technique is the best guarantee to find the global minimum since in the first stage a rather complete search is made over the complete parameter space. In most of the fits to real data we did, however, not find a clear global minimum.

In the χ^2-minimization procedure we implemented data on cross-sections and spin observables for different strangeness producing reactions.

4. Stability of fitting calculations

As a first check of the reliability of the fitting procedure, we have applied it to a set of 'data' points generated by our own calculation. An exact 'fit' is thus possible with $\chi^2 = 0$ and we check how often we reach this. Among other things this procedure allows us to test the uniqueness of the results. Obviously, there are several sign ambiguities in the parameters. Changing the signs of all coupling constants for a given resonance will leave the matrix elements invariant. This sign ambiguity is removed by defining certain parameters to be positive.

From these test runs we found that

- Our minimization procedure is able to recover the input parameters.
- Only about 5–10% of minimization runs reach a χ^2 close to 0.
- The genetic fitting step is vital in the fitting process as the gradient minimizer has a tendency to get stuck in the local minima.

To make the test case more realistic we have added Gaussian noise to our fake data. The best fit should now have $\chi^2 = 1$. Of the 75 attempted fits there are 6 calculations with χ^2/N (χ^2/data point) less than 1.2. It should be noted that in general, the polarization observables show the largest deviations. All these six calculations converge to the same parameter set which shows the stability of the fit procedure.

It is worth noting that convergence rate for the 'noisy' fits is compatible with the exact ones. This – at first – surprising result is caused by the large non-linearity of the problem. The χ^2-surface has many local minima and the second stage fit only converges to a good minimum if the genetic algorithm came close enough.

5. Results

From the SAPHIR experiment [23,24] we have data on differential cross-sections and recoil polarizations for $\gamma + p \to K^+ + \Lambda$, $\to K^+ + \Sigma^0$ and $\to K^0 + \Sigma^+$. As a first trial in fitting the SAPHIR data, we performed 200 rounds of GA + DN2FB fitting with 24 free parameters. About 30% of the calculations have converged well to a total χ^2 per data point of below 2 which is a high percentage compared to the fits discussed in the previous section. It is interesting to note that a large number of calculations have converged to the two lowest minima (10 and 20% respectively of the well-converged ones). The other good calculations converged to different local minima.

Figure 1 shows the resulting χ^2 and parameter values as extracted by a Minuit run on a subset of converged calculations. The error bars on the parameters are taken from the Minuit run and should reflect one standard deviation. The first two results in this set correspond to the above-mentioned two best minima (which had a large number of calculations converged to it), and the rest are a random selection from the other converged calculations.

All the presented results have comparable total χ^2. Also the partial χ^2 values for the fits to the differential cross-sections are comparable. The large variations are seen in the fits to the recoil polarizations for the different reactions and the fits

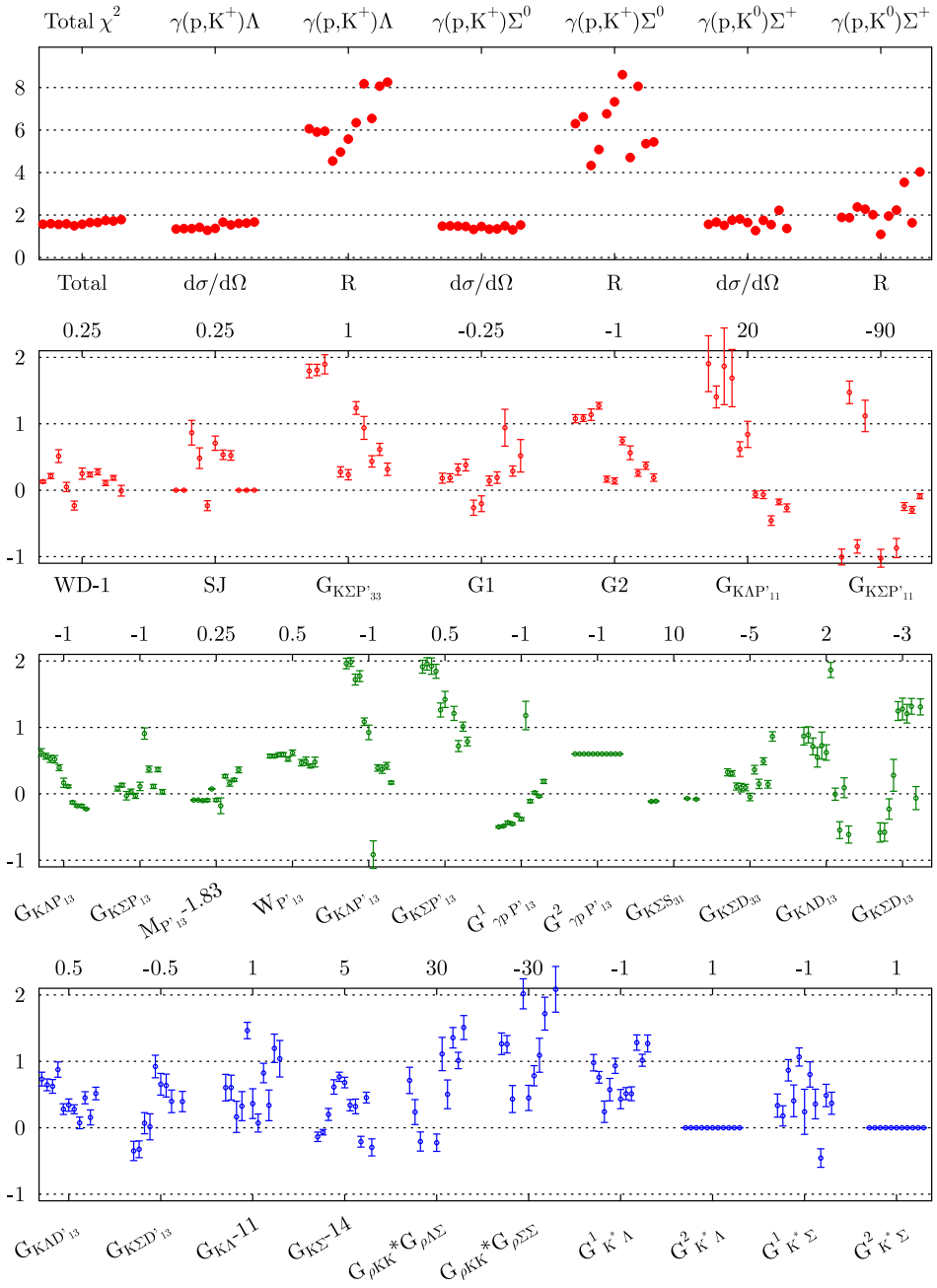

Figure 1. Model parameters and χ^2-values as obtained from fits to the data from the SAPHIR Collaboration. The top panel lists the values of the total and partial χ^2 values. The lower three show the extracted values of the parameters in the Lagrangian. The range multiplier for the values is given on top, the name of the parameter below.

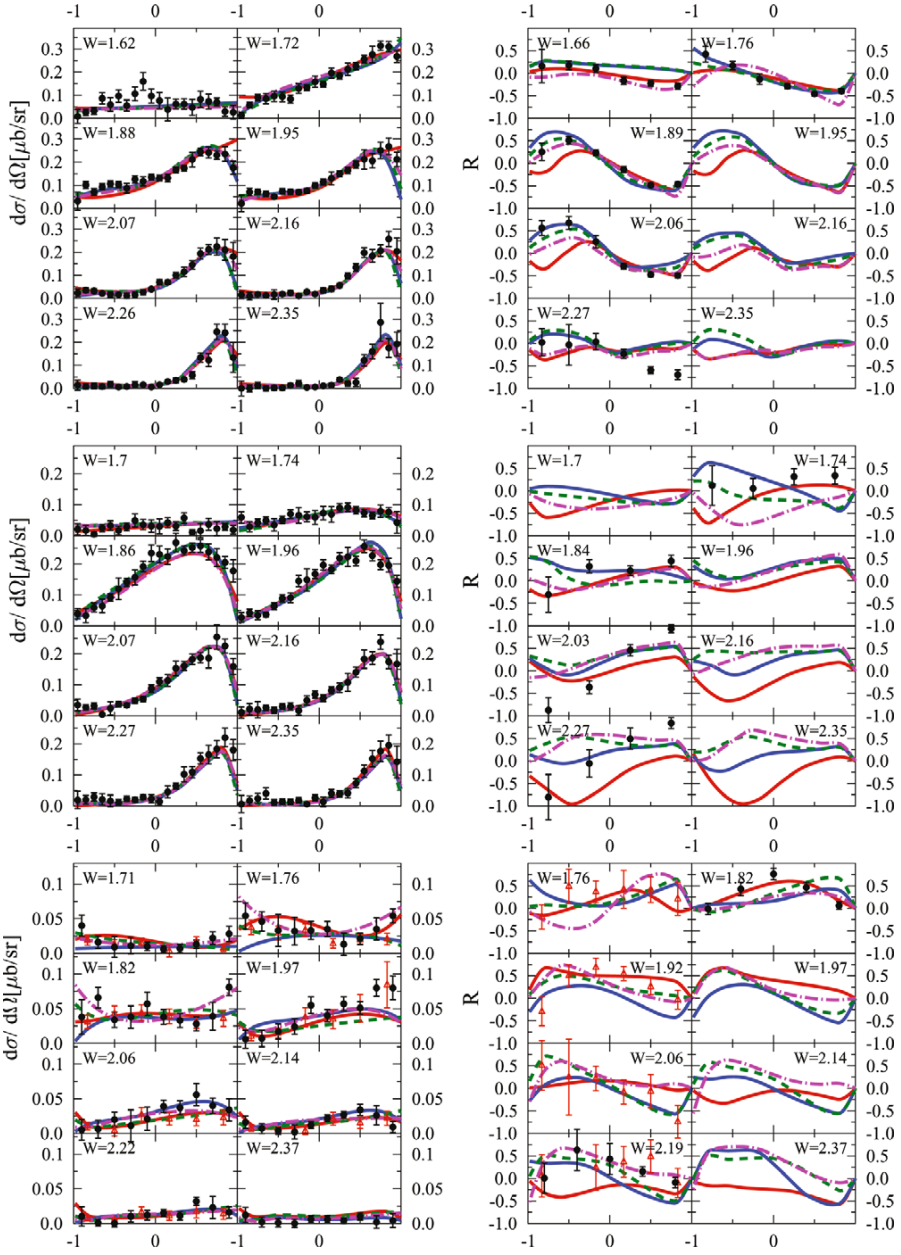

Figure 2. The results of some of the fitting calculations are compared to the data from the SAPHIR Collaboration.

are considerably worse. To some extent this is due to the fact that there are fewer data points for the recoil polarizations and as a result a poorer fit does not greatly affect the total χ^2. The lower three segments of figure 1 show the extracted parameters. The complete structure of the Lagrangian is given in ref. [2] and here

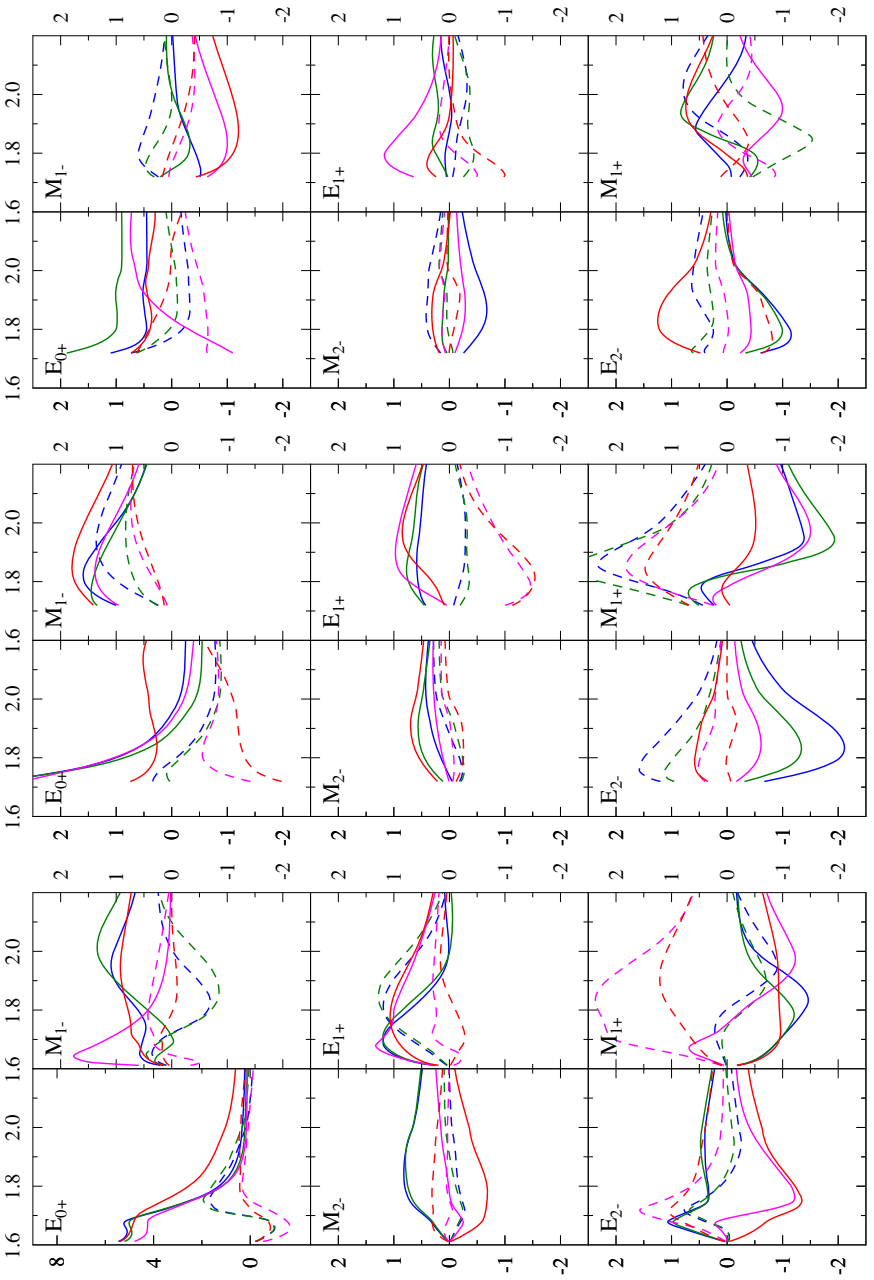

Figure 3. Partial wave amplitudes as obtained from fits to the data from the SAPHIR Collaboration.

we will mention only few of them. WD_1 and SJ in figure 1 are related to contact terms that determine the deviation from the usual DW formulation for restoring gauge invariance and as can be seen the deviation is small for most fits. Certain parameters, notably all P'_{33} parameters, the Λ coupling of D'_{13}, $g_{K\Lambda}$, $g_{K\Sigma}$ are rather uniquely defined by the fit. However, some of the others vary greatly, such as the coupling strengths for the P'_{13} and P'_{11} resonances. Some of the listed parameters are the products of two coupling constants as they enter in the photoproduction reaction, in particular $G1 = G_{KS}^{P'_{33}} \times G_{g_1N}^{P'_{33}}$ and similar for $G2$. Some of the parameters obtained values close to the limits set in the fit such as some of the couplings for the P'_{11}-resonance and the $g_{\rho\Sigma\Sigma}$ coupling. These large values for the coupling strengths signal that either the corresponding contributions are only indirectly affecting the calculated observables through some higher-order rescattering process, or that the coupling is not affecting the particular dataset that has been selected for the present calculations.

From all fit results four calculations were selected for a closer examination (can be seen from figure 2) and all give a rather good fit to the data and large differences are seen in the calculations for the recoil polarization. The reason for these larger differences for polarization observables is the relatively large error bars and the fact that they are bounded between -1 and $+1$ which gives them a relatively small leverage arm in the fit procedure. For the same reason, the chance of the fitting procedure to find the correct χ^2 minimum for these polarization observables is diminished.

Differences in model parameters do not necessarily imply that the calculations differ. Some parameters may not be independent and variations in one could be (almost) compensated by a variation in one or more parameters. In order to be able to investigate the actual differences between the different fits, we display in figure 3 the partial wave amplitudes for the different photoinduced strangeness-production channels. There are large variations in almost all partial waves with only the $E_{0+}(K\Lambda)$ and $M_{1+}(K\Sigma^0)$ as noticeable exceptions. This shows that to constrain the fit additional data for other polarization observables are necessary.

For the present calculations we have limited ourselves to the SAPHIR data since these have a complete set of recoil polarizations. Data are also available from the CLAS Collaboration [25,26] for differential cross-sections and some polarization data. Unfortunately the two experiments cannot be fitted simultaneously as many of the data on cross-sections differ more than the error bars would indicate.

6. Conclusions

We have shown that the K-matrix formalism offers a very powerful tool for a realistic analysis of meson–nucleon scattering. It gives a realistic account of rescattering effects by restoring unitarity of the S-matrix and still satisfying crossing symmetry and gauge invariance. At the same time, the formalism is simple enough to allow for a large-scale χ^2 fitting of the model parameters. In the fit more than 20 parameters are fitted to the collected data set differential cross-sections and polarization observables for a number of reactions. In spite of the extensive data set the resulting

partial wave decomposition was not unique with large ambiguities in most partial waves. Additional polarization observables are necessary to constrain the phases.

References

[1] A Usov and O Scholten, *Phys. Rev.* **C72**, 025205 (2005)
[2] A Usov and O Scholten, *Phys. Rev.* **C74**, 015205 (2006)
[3] A Yu Korchin, O Scholten and R G E Timmermans, *Phys. Lett.* **B438**, 1 (1998)
[4] G Penner and U Mosel, *Phys. Rev.* **C66**, 055211 (2002); **66**, 055212 (2002)
G Penner, *Vector meson production and nucleon resonance analysis in a coupled channel approach*, Ph.D. thesis (in English) (Universität Giessen, 2002), available at the URL http://theorie.physik.uni-giessen.de
[5] V Shklyar, H Lenske, U Mosel and G Penner, *Phys. Rev.* **C71**, 055206 (2005)
[6] S Kondratyuk and O Scholten, *Nucl. Phys.* **A677**, 396 (2000)
S Kondratyuk and O Scholten, *Phys. Rev.* **C62**, 025203 (2000)
[7] S Kondratyuk and O Scholten, *Phys. Rev.* **C65**, 038201; *ibid. Phys. Rev.* **C64**, 024005 (2001)
[8] T Sato and T-S H Lee, *Phys. Rev.* **C54**, 2660 (1996)
[9] M F M Lutz and E E Kolomeitsev, *Nucl. Phys.* **A700**, 193 (2002)
[10] O Scholten *et al*, *Acta Phys. Pol.* **B33**, 847 (2002)
[11] R Shyam and O Scholten, *Phys. Rev.* **C78**, 065201 (2008)
[12] S Ozaki *et al*, *Phys. Rev.* **C80**, 035201 (2009)
[13] A Yu Korchin and O Scholten, *Phys. Rev.* **C68**, 045206 (2003)
[14] R M Davidson and R Workman, *Phys. Rev.* **C63**, 025210 (2001)
[15] M Benmerrouche, N C Mukhopadhyay and J F Zhang, *Phys. Rev.* **D51**, 3237 (1995)
N C Mukhopadhyay and N Mathur, *Phys. Lett.* **B444**, 7 (1998)
R M Davidson, N Mathur and N C Mukhopadhyay, *Phys. Rev.* **C62**, 058201 (2000)
[16] R Workman, R A Arndt and I I Strakovsky, *Phys. Rev.* **C62**, 048201 (2000)
R A Arndt, W J Briscoe, I I Strakovsky and R L Workman, *Phys. Rev.* **C66**, 055213 (2002)
Ya I Azimov, R A Arndt, I I Strakovsky and R L Workman, *Phys. Rev.* **C68**, 045204 (2003)
R A Arndt, W J Briscoe, I I Strakovsky and R L Workman, *Phys. Rev.* **C72**, 058203 (2005)
[17] L Tiator, D Drechsel, G Knöchlein and C Bennhold, *Phys. Rev.* **C60**, 035210 (1999)
[18] D Drechsel, O Hanstein, S S Kamalov and L Tiator, *Nucl. Phys.* **A645**, 145 (1999)
[19] R Shyam, *Phys. Rev.* **C75**, 055201 (2007)
R Shyam, *Phys. Rev.* **C60**, 055213 (1999)
R Shyam, G Penner and U Mosel, *Phys. Rev.* **C63**, 022202(R) (2001)
R Shyam, *Phys. Rev.* **C73**, 035211 (2006)
[20] Stijn Janssen, Jan Ryckbusch, Dimitri Debruyne and Tim Van Cauteren, *Phys. Rev.* **C65**, 015201 (2001)
[21] D G Ireland, S Janssen and J Ryckebusch, *Nucl. Phys.* **A740**, 147 (2004)
[22] The PORT3 library I used is available from the URL http://www.netlib.org/port/readme
[23] K H Glander *et al*, *Eur. Phys. J.* **A19**, 251 (2004)
[24] R Lawall *et al*, *Eur. Phys. J.* **A24**, 275 (2005)
[25] R Bradford *et al*, *Phys. Rev.* **C73**, 035202 (2006)
R A Schumacher, Private communication (2009)
[26] J W C McNabb *et al*, *Phys. Rev.* **C69**, 042201 (2004)